Title:

Data-driven analysis of rat pup behavior reveals novel effects of maternal pre-conception exposure to nicotine.

Authors:

Reza Torabi[1], Serena Jenkins[1], Allonna Harker, Ian Q. Whishaw, Robbin Gibb, Artur Luczak*

Canadian Center for Behavioural Neuroscience, University of Lethbridge, 4401 University dr., Lethbridge, AB, Canada

[1] equal contribution.

* Corresponding author: Luczak@uleth.ca

Abstract

We present a deep neural network for data-driven analyses of infant rat behavior in an open field task. The network was applied to study the effect of maternal nicotine exposure prior to conception on offspring motor development. The neural network outperformed human expert designed animal locomotion measures in distinguishing rat pups born of preconception nicotine dams versus control dams. Notably, the network discovered novel movement alterations in posture, movement initiation and a stereotypy in "warm-up" behavior (repetition of movement along specific dimensions) that were the most predictive of nicotine exposure. This suggests that maternal preconception nicotine exposure delays and alters offspring motor development. In summary, we demonstrated that a deep neural network can automatically assess animal behavior with high accuracy, and that it offers a novel, data-driven approach to investigating brain alterations in development.

Keywords: Data driven analysis, animal behavior, post-natal development, maternal preconception nicotine

Abbreviations: MPNE: maternal preconception nicotine exposure

Introduction

Animal behavior is a sensitive indicator of brain function and behavioral observation and in addition to being relatively non-invasive, is central to documenting normal and altered brain activity[1-7]. For example, open field exploratory behavioral measures are used to detect changes associated with neurological disorders, pharmacological treatments or environmental conditions[8]. Consequently, many methods and tools have been introduced in order to quantify this behavior[8-18]. These methods typically require that an experienced observer identifies behavioral abnormalities and designs quantifying measures, which can be time consuming and human designed measures are often sub-optimal due to inherent difficulty of quantifying complex behavior[19]. To reduce this problem, we introduce a deep neural network that automatically classifies spontaneous behavior and extracts, in a data-driven way, movements that distinguish control and experimental groups of animals.

We applied our network to study the effect of maternal preconception nicotine exposure (MPNE) on rat offspring locomotor development in an open field task[20,21]. Developmental nicotine exposure is frequently associated with changes in locomotor activity. In humans, smoking during pregnancy predicts the prevalence of ADHD symptoms in school-aged children after controlling for demographic factors[22]. In an animal model of nicotine exposure, prenatal nicotine is found to be associated with hyperactivity[23]. For example, Zhu and colleagues exposed F0 female mice to 0.1mg/ml in their drinking water for three weeks prior to and throughout pregnancy and found that not only are the F1 offspring hyperactive in early adulthood[24], but the effect propagates down the maternal line such that the F2 and F3 offspring are hyperactive relative to controls as well[25]. Some studies have examined the impact of preconception paternal nicotine exposure on offspring locomotor activity and have similarly found increased activity in F1 young adult offspring[26]. Nicotine may induce hyperactivity due to its ability to down-regulate the dopaminergic and adrenergic neurotransmitter systems that are implicated in the etiology of ADHD[27]. Nevertheless, others have found, when examining pre-weanling pups (postnatal day (P)19), that prenatal nicotine decreases locomotor activity relative to control animals in an open field[28].

Because the consequences of MPNE on offspring development are likely to be subtle and vary due to developmental age and the selection of behavioral tests and their measurement, more sensitive

behavioral measures could prove useful. For example, the DSM-5 criteria for the diagnosis of ADHD consists of end point measures of the extent to which intrusive activity interrupts behavior in a number of school/home/work settings. Animal models of ADHD similarly use end point measures of open field or swim tests to assess behavioral disruption. We present a new data-driven analysis method to identify MPNE rat pup behavioral changes in an open field task and so provide a better understanding of the neuropharmacological effects of nicotine on brain development. The current research addresses two gaps in our understanding of nicotine's impact on locomotor activity. First, does nicotine administration during the preconception period in prospective dams, as opposed to the prenatal, preconception + prenatal, or paternal preconception period, affect behavior? Second, is offspring behavior affected at an early stage of development, thus demonstrating the immediate impact of MPNE on offspring locomotion?

To address those questions, we first analyzed animal video recordings using standard locomotor-derived kinematic measures in order to study an effect that MPNE has on infant rat behavior. Then we showed that a neural network can outperform this conventional analysis in identifying the effect of MPNE. Lastly, we extracted knowledge from the deep neural network in order to identify behavioral components that distinguished the nicotine exposed group from the control group. This data-driven analysis uncovered novel alterations in "warm-up"[29-31] behavior that provides new directions in examining the neural consequences of nicotine exposure. Thus, our method demonstrates a new approach to develop more sensitive behavioral measures for the detection and monitoring of neuropharmacological effects.

Results

Effect of maternal nicotine exposure prior to conception on offspring: analyses of behavior using expert selected measures.

Standard locomotor measures were used to investigate the effect of MPNE on offspring locomotor development [Methods]. Of 351 rat pups, 191 were from preconception sucralose-exposed dams, and 160 were from preconception nicotine-exposed dams [Methods]. When 10-days old (P10), pups were placed singly in the open field for one minute and their behavior was videotaped to investigate locomotor development [Methods]. The movement of an animal was described in terms of movement kinematics[20,21]: (1) Total activity - the total number of square entries for either front

paw of the animal during the exploration, and (2) Novel activity - the number of unique square entries, which relates to locomotor complexity. Those measures were calculated separately for the inner and outer part of the open field (Fig. 1A, Methods). A statistical comparison of the above movement measures of the MPNE (nicotine exposed dam) and control groups (sucralose-exposed dam) are shown in Fig. 1B. The MPNE group was less active, entered fewer squares and explored fewer novel squares than did the control group ($\text{Total}_{\text{Control}}$ = 57.0±1.8, $\text{Total}_{\text{Nicotine}}$ = 42.2±1.6; Total $\text{Inner}_{\text{Control}}$ = 32.0±1.2, Total $\text{Inner}_{\text{Nicotine}}$ = 26.4±2.0; Total $\text{Outer}_{\text{Control}}$ = 24.0±1.2, Total $\text{Outer}_{\text{Nicotine}}$ = 15.0±1.0; $\text{Novel}_{\text{Control}}$ = 21.0±0.6, $\text{Novel}_{\text{Nicotine}}$ = 15.5±0.6; Novel $\text{Inner}_{\text{Control}}$ = 11.1±0.4, Novel $\text{Inner}_{\text{Nicotine}}$ = 9.1±0.3; Novel $\text{Outer}_{\text{Control}}$ = 9.9±0.5, Novel $\text{Outer}_{\text{Nicotine}}$ = 6.3±0.3; "±" represents SEM; $p<0.001$ for all comparisons using *t*-test; using non-parametric Mann-Whitney U test also gave significant results for all comparisons with $p<0.003$). In summary, on all measures the MPNE offspring showed less exploration than the control offspring.

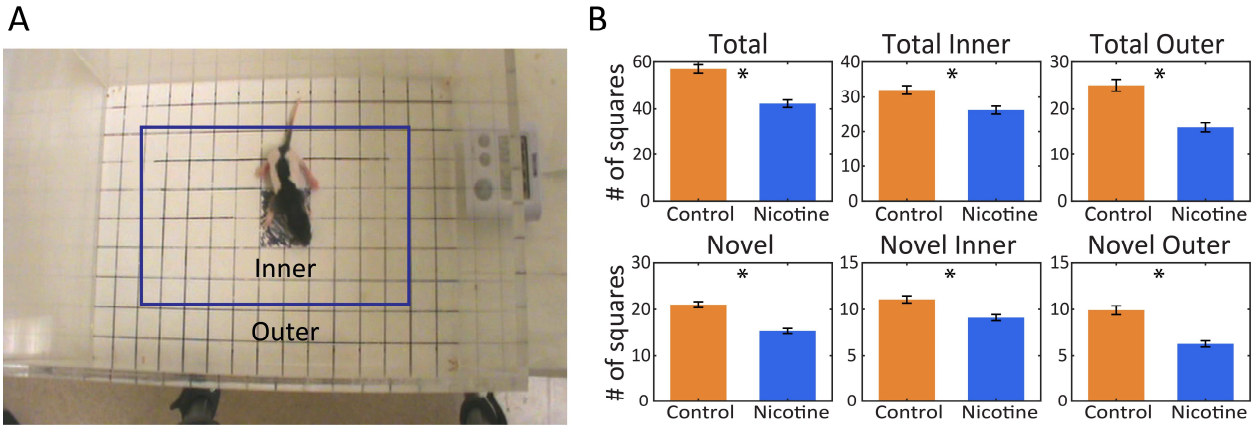

Fig. 1: Movement of 10-day old rat pups in open field task. (A) Definition of outer and inner portions of the open field. (B) Comparing movement measures in nicotine and control animals reveals significant effect of MPNE on offspring exploration (see Methods for measures description).

Combining movement measures to distinguish the control vs. nicotine groups

As described above, we quantified the behavior by using typical kinematic measures employed in an open field task. This approach requires assumptions regarding which features of the behavior will be useful in distinguishing between treatment groups. To estimate the reliability of these

expert selected features, we used machine learning algorithms to predict treatment group using all six values of behavioral measures described above. We used five different algorithms to ensure that our results are not dependent on a specific data analysis method. For all algorithms we used five-fold cross-validation, where we trained the model on 80% of trials and predicted treatment group for the remaining 20% of trials. We repeated this process 5 times to predict group category for every trial. The algorithms discriminated between the two groups with accuracy between 57-72% (Decision tree: 57%; Random forest: 61%; Logistic regression: 61%; K-nearest neighbors: 63%; Support vector machine: 72%) [Methods]. This means that based on described movement measures it is possible to tell with about 72% accuracy if it is a control or nicotine group animal (chance level is 50%). We then applied principle component analysis (PCA) to the movement measures. The distribution of points for both classes largely overlapped in PC space (Suppl. Fig. 1). It indicates a weak discriminability between classes, which is consistent with the above result using machine learning algorithms.

Using deep neural network to distinguish the control vs. nicotine groups

To investigate if additional information could be extracted from the rat pup's behavior, we used a deep neural network to examine the same videos of MPNE and control animals in the open field task [Fig. 2A, Methods]. This approach does not require specifying which behavioral measures should be used. Rather, the neural network discovers by itself which features in video (e.g. shapes, movements, etc.) are the most predictive of the treatment groups. The neural network design was based on our previous network[32]; specifically, we used a convolutional network (ConvNet)[33] to convert each video frame (400×350 pixels) to a set of 2048 features. Those features may loosely correspond to object edges. Features from 150 video frames from a single video clip were then combined and passed to a recurrent neural network (RNN). This allowed an analysis of animal movements throughout each trial (1 trial = 1 video clip consisting of 150 frames corresponding to 50 sec). The network was then trained to assign a correct group category to each video clip (Fig. 2A, Methods), and then information was extracted from the network to investigate its decision making (Fig. 2B, see next section).

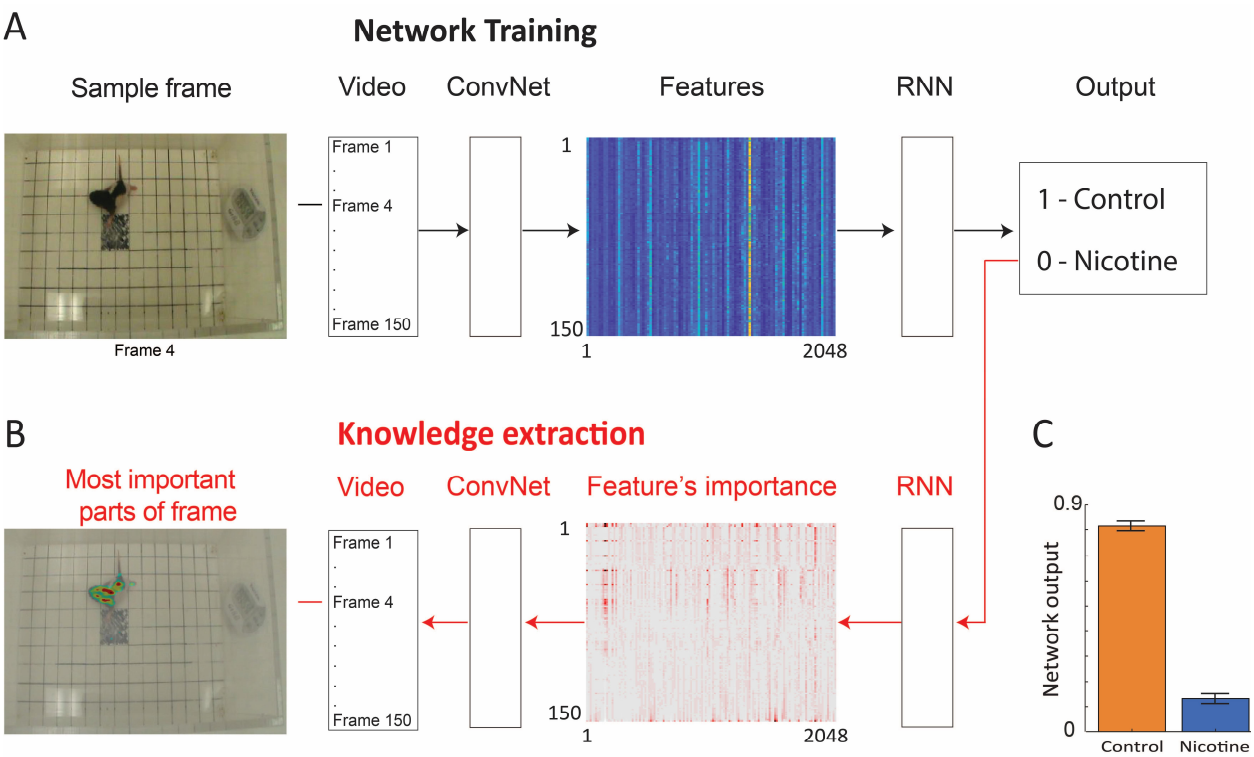

Fig. 2: Neural network architecture for data-driven analyses. (A) The network is trained using video clips of single trials (each consisting of 150 video frames). Frames are then passed through a convolutional network (ConvNet) to extract 2048 high level image features from each frame. The features from 150 successive video frames are then given as an input to a recurrent neural network (RNN) to analyze temporal information across frames. Based on this information, RNN predicts for each video clip a group category (Output). (B) After the network is trained, information is extracted from the network weights in order to identify image features and the parts of each video frame that were the most important for network decision making. For visualization, only every 20th feature is shown. (C) Average activity of the output neuron for animal videos from each group.

After training, the network was able to distinguish videos of the MPNE and control groups with 87% accuracy. This accuracy is considerably higher than the classification accuracy obtained from kinematic defined movement features (57%-72%). Fig. 2C shows the average activity of the output neuron for the control group (mean = 0.82±0.02 SEM) and the nicotine group (mean = 0.13±0.017 SEM). The activity of the output neuron was bounded between 0-1, with 1 corresponding to the

control category. For example, a value of the output neuron of 0.9 can be interpreted as the network is 90% 'confident' that it is a control animal, and only 10% 'confident' that it is a MPNE animal. For calculating the network's prediction accuracy, values of the output neuron above 0.5 was considered as control group, and values below 0.5 as the MPNE group.

To verify that our network does not require fine parameter tuning for robust performance, we also tested four variations of the network. In particular, we modified the number of neurons and layers in the RNN, and we repeated the training and testing on the same data. The modified networks produced results similar to those of the original network (Suppl. Fig. 2). To ensure that network accuracy is not a result of an overfitting and that our network can generalize to new animals, all predictions were obtained using five-fold cross-validation as described above. Thus, no videos of the predicted animal were included in the training dataset. Altogether, these results indicate that there is information about MPNE in the behavior that is not accounted for by the standard movement analyses.

Extracting knowledge from the neural network

Considering that the network classified the animal groups from videos with higher accuracy than kinematic measures, we investigated what movement features were the most informative for the network. We applied a recently developed Layer-wise Relevance Propagation method (LRP) to extract knowledge from deep neural networks[34,35] [Methods; Suppl. Text 1]. First, we identified which features extracted from the videos were contributing the most to the predictions made by the RNN (Fig. 2B – features importance array), and then we found which parts of each frame corresponded to those most informative features (Fig. 2B – left side). Thus, knowledge extraction reveals the network's focus for decision making.

Examination of the feature's importance matrix revealed that certain video frames were particularly informative for the network decision. For example, the first frames had multiple features which contributed to network classification more strongly than subsequent frames (Fig. 3A, Suppl. Fig 3). Plotting the average value of the features separately for each animal group showed the high discriminative power of those initial frames (Fig. 3B). To investigate why, we closely inspected those first frames. We found that on average, there was a meaningful difference in the starting posture and starting movement between the MPNE and control animals. Fig. 3C,D

illustrates the difference in their starting posture as soon as the experimenter placed the pups in the open field box. The MPNE animals sprawled, with the fore and hind legs extended, whereas the control animals had their limbs beneath them. In short, the MPNE animals displayed reduced postural support. The lack of postural support indicated by extended limbs could also be observed as the MPNE animals initiated movement. The temporal features of movement were also different between MNPE and control animals as the control animals started to move as soon as they were placed in the open field. They collected their body by bringing their limbs to a weight bearing posture and made small movements of their head as they initiated movement. The MPNE animals mostly lingered (not moving), taking more time to establish postural support and then initiated movement.

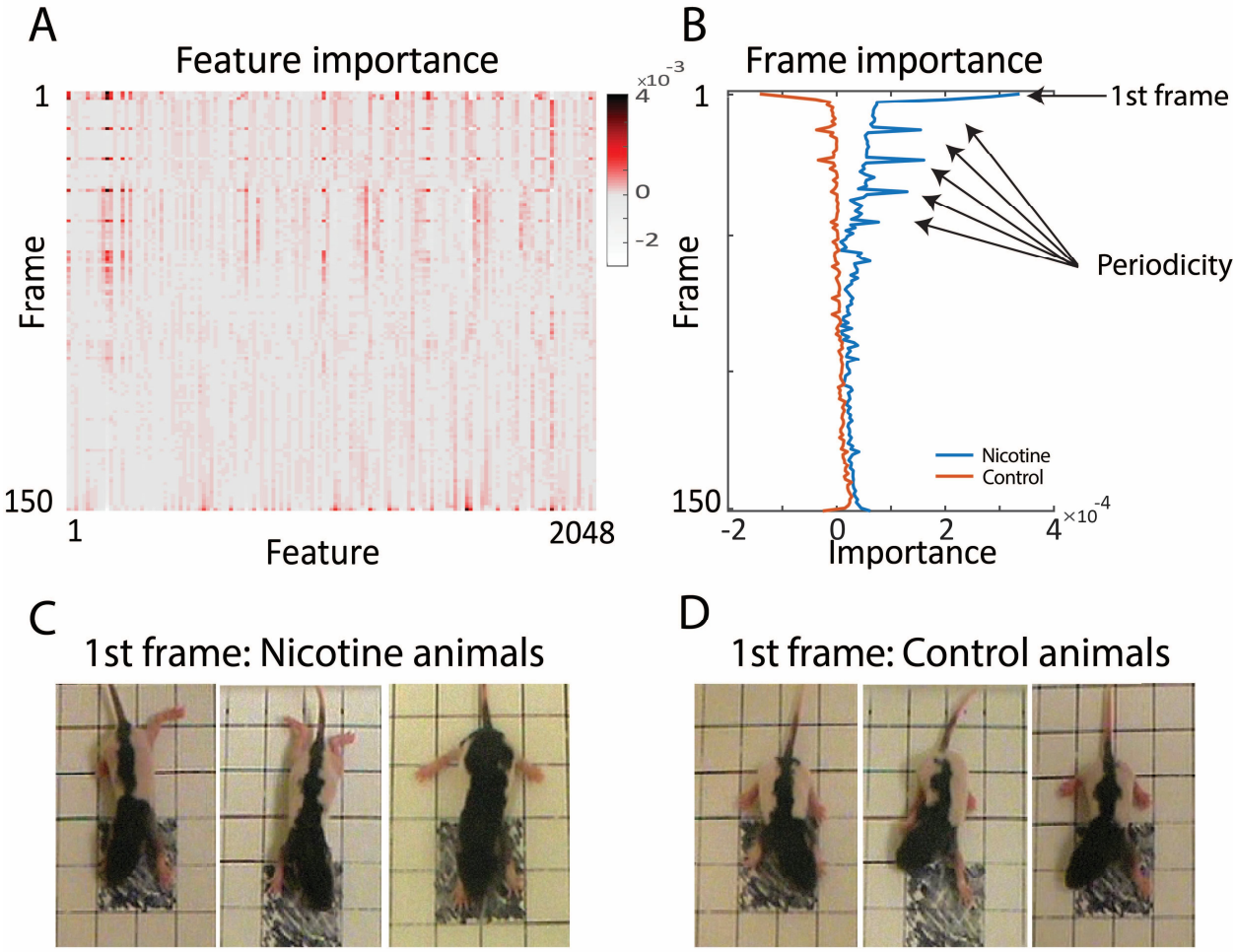

Fig. 3: Finding the most informative behavioral features used by the network for decision making. (A) Average feature importance over all videos. (B) Average importance of each video frame,

for each animal group. This revealed that the 1st frame and every 11th frame were particularly important. (C & D) Typical starting postures (1st frame) of MPNE (C) and control animals (D). Examples of 3 rats from each group are shown. For visualization clarity, only the portion of frame with the pup is shown. Note extended legs in the MPNE group, and collected legs supporting weight in the control group.

Visualization of feature importance also showed unexpected periodic changes (Fig. 3B). Specifically, features occurring about every 11th frame, corresponding to period of about 3.7 sec, are particularly informative for the network's distinction between the MPNE and control groups. This was also confirmed with spectral analyses shown in Suppl. Fig. 4 & 5. To investigate the behavior underlying the distinguishing movements, we divided the videos into 11 frame segments and aligned the segments (Fig. 4). This revealed a stereotypical, repetitive behavior in MPNE animals. The animals made repeated lateral movements that returned the animal to its initial position. For comparison, Fig. 5 illustrates a typical temporal sequence of two control animals at the same time. The control animals also make lateral movements, but the amplitude and frequency of movement are different from that of the MPNE animals. For example, in the control rat #1, the lateral head movement begins at frame 10 and it ends at frame 18. Its next lateral movement increases in amplitude, thus modifying the sequence of movement (i.e. frames 21 and 31 are not the same in Fig 5 for rat #1). Moreover, some of the control animals pivoted as part of the lateral movement (Fig 5, rat #2).

Note that although our analyses showed that features of importance peak at frames 10, 21, …, etc., it should not be interpreted that only those specific frames are of significance to the network. Rather, it should be seen as an indication that at those times the network recognized a specific stereotypical sequence. Thus, the network identified from raw video data the stereotypical behavior as a distinguishing feature of MPNE pups.

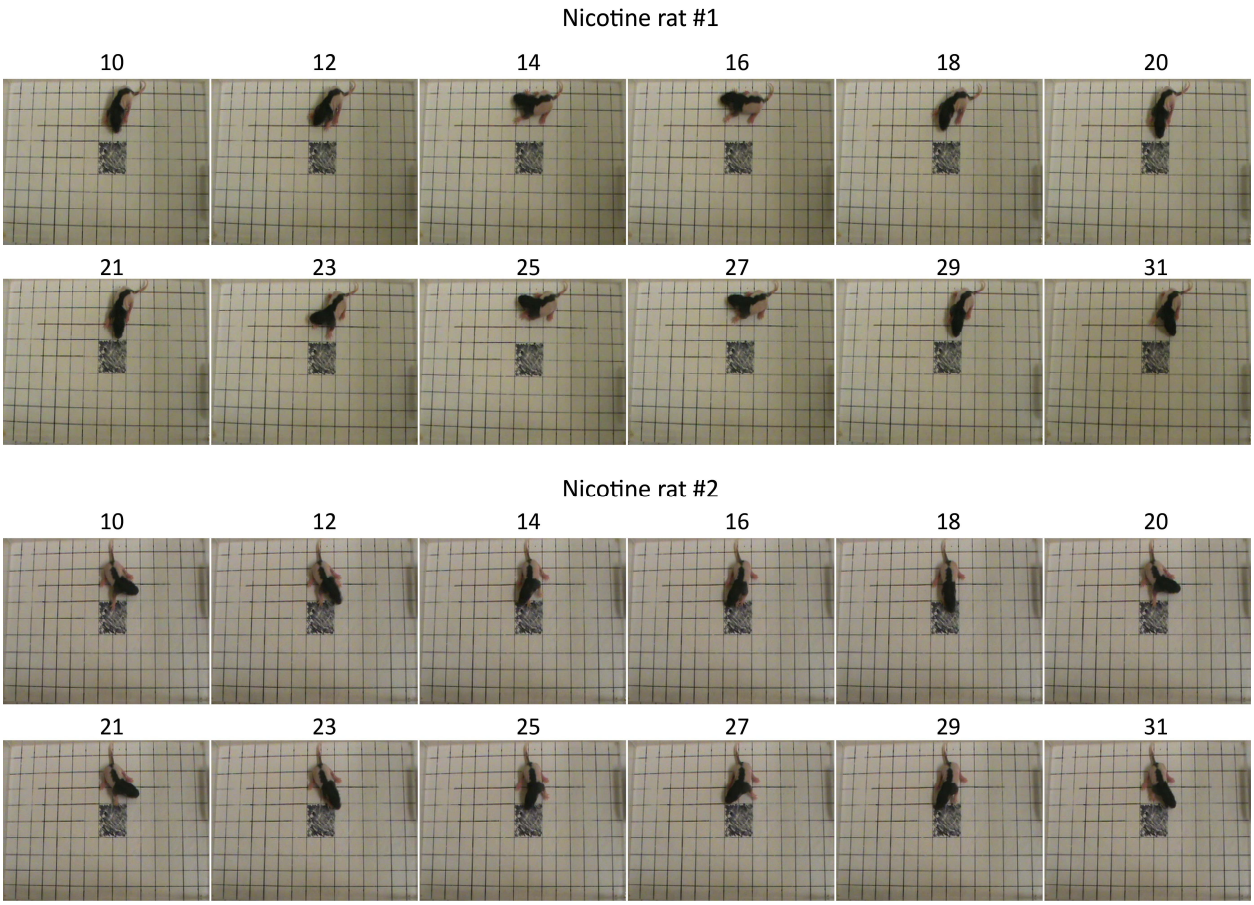

Fig. 4: Stereotypical behavior in two rat pups from the MPNE group. Numbers above the pictures represent the frame number. Note the almost exact same body position every 11 frames.

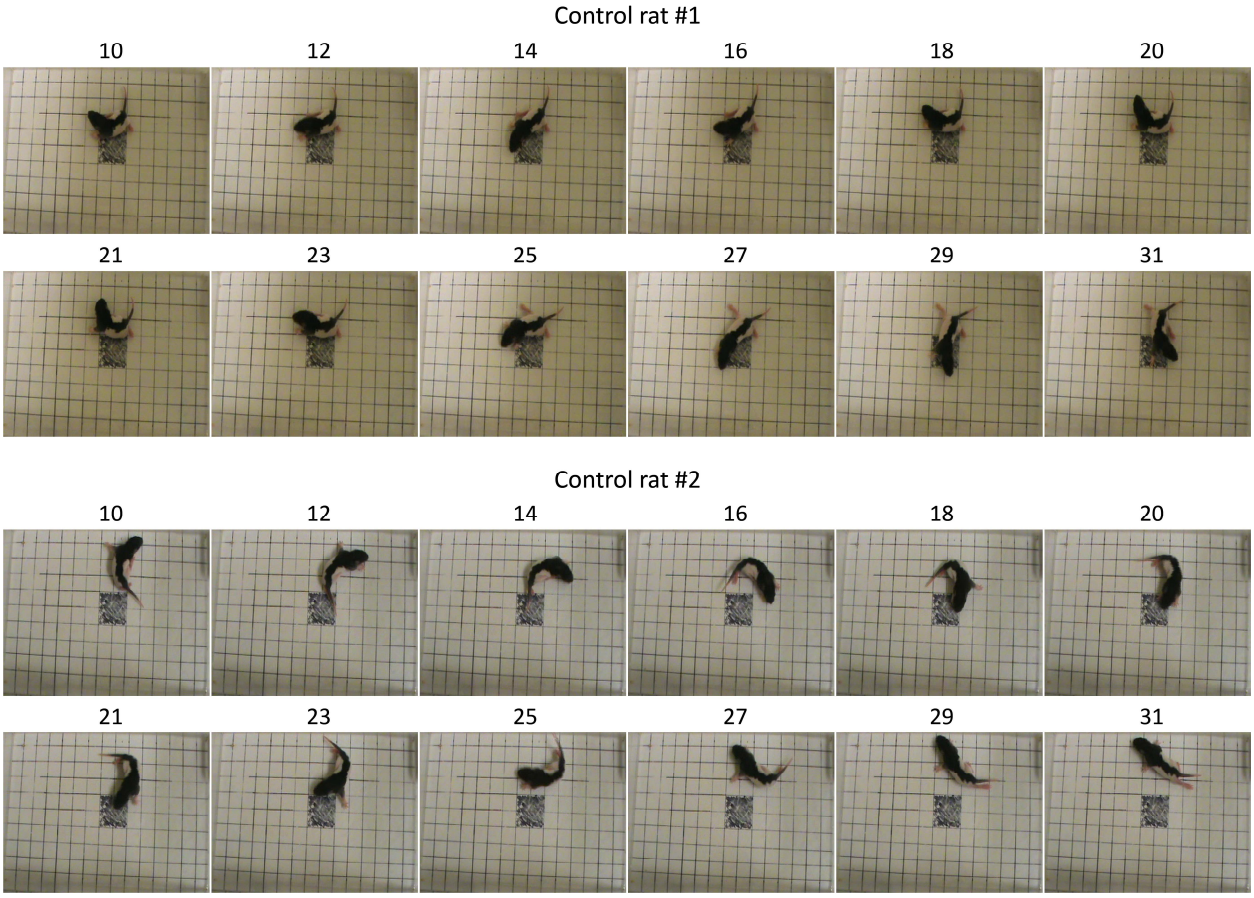

Fig. 5: Sample behavior of typical control animals. The movements are less repetitive compared to nicotine animals and more diverse as exemplified by pivoting (rat #2).

Discussion

The neural network described here provides a state-of-the-art method for automated behavior analyses. The use of a data-driven approach to behavioral analysis offers three advantages. First, it saves researcher time as there is no need for time-consuming human scoring of movement. Second, it increases accuracy, as it explicitly identifies behavioral features that differentiate treatment groups. Third, the largest advantage of the network is that it offers a powerful data-driven approach to gain new insights into behavior. For example, only after looking at feature importance provided by the network did we notice that MPNE pups display altered posture and stereotyped movements that can be diagnosed as early as the first few video frames. Thus, by analyzing the network's decision-making process, new insights into behavioral differences are

obtained. Considering that quantifying behavior is central to most neuroscience research, the method presented here has significant applicability.

Comparison with other methods

One approach to improving the analysis of exploratory behavior is the use of tracking systems using markers that are automatically or manually attached to body parts[36]. In the last few years several methods such as LocoMouse[8], DeepLabCut[9], JABAA[10], Optimouse[11], and LEAP[12] have been developed to allow users to identify key points in videos, such as the location of a paw, and then it automatically tracks the movement of those key points across video frames. For instance, in DeepLabCut[9], the experimenter manually labels body parts (e.g. the snout, left ear, right ear, tail) in selected video frames using virtual markers, and then the network is trained to automatically predict the position of those body parts in the rest of the video. Although this method is useful, it requires investigator decisions about relevant body parts, and it requires separate analyses to determine whether the measures are relevant.

The second category of automated methods such as MoSeq[14] and MotionMapper[15] first reduce the dimensionality of the video data, and then relate the results to the behavioral components. These methods require image pre-processing and proper image alignment, and additional methods must be applied for classifications. Our method offers an alternative to both of these approaches. First, the convolutional network works with raw images without the need of pre-processing and without the difficult task of image alignment, and second, the network automatically identifies the most relevant behavior for predictions. In short, it offers a one-step solution for feature selection and animal group classification.

Significance of behavioral results

Our data-driven approach identified impaired postural support and increased stereotypical behavior as prominent features of the pups of maternal preconception nicotine exposed (MPNE) mothers. One interpretation of these results is that the MPNE offspring are developmentally delayed compared to the control offspring. One line of research has identified “warm-up” as a key feature of animal movement development. When an animal is placed in a novel location,

movement initiation is organized with lateral, forward and dorsoventral movements emerging sequentially and then escalating in amplitude into forward locomotion[29,30]. Warm-up is also a feature of the ontogeny of motor development in which the topography and amplitude of movement emerges as maturation proceeds[29]. According to this view, the MPNE animals are motorically underdeveloped relative to the control animals in that their reduced postural support is diagnostic of a lower level of maturation relative to control pups.

Another interpretation of our results is that MPNE differentially effects subsystems of movement that support posture vs locomotion. For example, in a pharmacological dissection of movement, DeRyck and Teitelbaum[37] found that morphine induced catalepsy features and poor postural support that is not incompatible with locomotion. According to this interpretation, the hyperactivity of ADHD in animal models is a symptom of the substitution of abnormal locomotor activity for impaired normal immobility. Given weaknesses in postural support mechanisms, the MPNE animals substitute stereotyped movement for normal locomotion[38-44].

Our exemplar study was limited to rat pups on postnatal day 10, but other work has featured the analysis of nicotine effects in animals at a variety of ages, with findings that locomotion is sometimes reduced neonatally and sometimes increased in adolescence and adulthood. [18,28] Our work suggests that future work could consider altered posture and stereotypical behaviors as contributors to the symptoms of nicotine exposure more generally. Of course, the application of our data-driven approach may yet uncover other features of age-dependent nicotine exposure that have not yet been described.

Methods

Animals

All procedures were conducted in accordance with the Canadian Council of Animal Care and were approved by the University of Lethbridge Animal Care and Use committee. Animals were given food and water ad libitum and were maintained on a 12-h light/dark schedule (lights on from 07:30 to 19:30) in a temperature- and humidity-controlled (21°/50%) breeding room. Female Long Evans rats (n = 23) were bred in-house and received 15mg/L nicotine hydrogen tartrate salt (Sigma) in their drinking water sweetened with 1% sucralose. Control dams (n = 22) received sucralose only. Nicotine was administered for seven consecutive weeks beginning in adulthood (90-days-old);

seven weeks is the length of the spermatogenic cycle in male Long Evans rats and was chosen to mirror the complementary paternal studies. On average, nicotine-exposed dams consumed 2.4mg of nicotine per kg of body weight per day across the seven weeks. Females were bred with non-drug-exposed male Long Evans rats the day following completion of nicotine administration. Animals in this analysis were 10-day-old rat pups from 32 successful litters for a total of 351 pups. Eighteen litters (191 pups: 102 female and 89 male) of the animals were from sucralose-exposed dams, and 14 litters (160 pups: 76 female and 84 male) were from nicotine-exposed dams.

Behavioral testing

Pups were tested in the open field task. The testing apparatus was a clear Plexiglas box measuring 10 in × 15 in with a grid of 150 squares on the floor with a size of 1 in ×1 in. Each day, pups were placed individually in the center four squares (shaded black) and left to explore the box for 1 min while being recorded from above. The open field was cleaned with Virkon between animals.
Kinematic movement measures and their definitions in scoring procedure are as follow:
Novel = the number of unique squares that either front paw of the pup enters, up to a maximum of 146 (i.e. the box is divided into 150 squares total (10×15), minus the four shaded squares).
Total = the total number of square entries for either front paw (i.e. the number of times a front paw goes from one square to another)
Novel Inner = the number of unique squares in the inner portion of the field that either front paw of the pup enters. (i.e. the number that are within the 6×11 squares in the center of the box, minus the four shaded squares).
Novel Outer = the number of unique squares in the outer portion that either front paw of the pup enters. (i.e. the two rows of squares that make up the perimeter of the open field)
Total Inner = the total number of square entries in the inner portion for either front paw.
Total Outer = the total number of square entries in the outer portion for either front paw.

Applying machine learning algorithms on movement measures
We used five different machine learning methods (logistic regression; decision tree; random forest; k-nearest neighbors; support vector machine) to see how well the movement measures could discriminate between the two groups of animals. In k-nearest method, we tried a different number of nearest neighbors to find the best accuracy. The best accuracy was found for k = 25 (‘k’ is the

number of neighbors). In random forest algorithm, the best accuracy was obtained with the number of ensembles n = 50. In SVM, the accuracy with its default parameters is 58%. However, we used grid search for tuning the hyper parameters (C and Gamma) as well as the kernel type to find the best accuracy. The best accuracy was found for C =1, Gamma = 0.01, and polynomial kernel with degree 2.

Deep Neural Network training and architecture

For training the neural network we used 351 videos: 160 from MPNE animals, and 191 videos from control animals. The original frame rate was 30 frames per second with resolutions 720×480 pixels. However, to reduce the amount of data, we used only every 10th video frame (3 per sec), and only 150 frames (50 sec) from each video.

The general network architecture is shown in Fig. 2. First, a pre-trained convolutional neural network (ConvNet) known as Inception-V3[33] was used to extract 2048 features from each video frame. This reduced each video to a 2D matrix of the size (2048 features ×150 frames). This matrix was then given as an input to the recurrent neural network (RNN) to predict animal groups. We used a RNN composed of 256 long short-term memory (LSTM) units in the first layer, followed by a dropout layer of 0.2 to prevent overfitting, and then a dense layer with two neurons with the softmax activation function to classify the animal's behavior. We used "Group K-Fold" in Keras to split the data randomly and uniformly (to prevent the train and test data being biased) into 5 classes. Batch size was 100 and Adam optimizer has been used with binary cross entropy as the loss function. Learning curve for the network is shown in Suppl. Fig 2B. The code for our network including all parameters is available in the Github repository as Behaviour_Recognizer toolbox: https://github.com/rezatorabi13/Behaviour_Recognizer.

Knowledge extraction method

After the network was trained, information was extracted from the network weights in order to identify image features and the parts of each video frame that most contributed to the network decision. For this knowledge extraction from the network, we used the Layer-wise Relevance Propagation method (LPR)[34,35] available in the DeepExplain package[45]. This method uses the strength of synaptic weights and neuronal activity in the previous layer to recursively calculate the

contribution (importance) of each neuron to the output score. Because our network is composed of two parts, ConvNet and RNN (Fig. 2A), we first investigated which features were most informative for the RNN to classify animal groups (Fig. 2B middle panel). Next, we propagated feature importance back to pixels in the video through the Inception V3 network (Fig. 2B left panel; Suppl. Fig. 6). This provided us with information as to which parts of the image the network was 'attending to' when making classification. This provided a sanity check that the network is indeed using rat movements rather than spurious features, such as the amount of lighting, to discriminate between the treatment groups. Using other methods for knowledge extraction like gradient*input methods[46,47] gave qualitatively similar results.

Acknowledgement

We thank A. Mashhoori, H. Ryait, N. Afrashteh, M. Ello, R. Zabair and J. Karimi for helpful comments. This work was supported by CIHR and NSERC DG to AL.

References

1 Eilam, D., Zor, R., Fineberg, N. & Hermesh, H. Animal behavior as a conceptual framework for the study of obsessive-compulsive disorder (OCD). *Behavioural Brain Research* **231**, 289-296, doi:10.1016/j.bbr.2011.06.033 (2012).

2 Zor, R. *et al.* Obsessive-compulsive disorder: a disorder of pessimal (non-functional) motor behavior. *Acta Psychiatr Scand* **120**, 288-298, doi:10.1111/j.1600-0447.2009.01370.x (2009).

3 Cenci, M. A., Francardo, V., O'Sullivan, S. S. & Lindgren, H. S. Rodent models of impulsive-compulsive behaviors in Parkinson's disease: How far have we reached? **82**, 561-573, doi:10.1016/j.nbd.2015.08.026 (2015).

4 Fouad, K., Torres-Espín, A. & Fenrich, K. K. Mechanisms of behavioral changes after spinal cord injury. *Oxford Research Encyclopedia of Neuroscience*, doi:10.1093/acrefore/9780190264086.013.245 (2019).

5 Bresnahan, J. C., Beattie, M. S., Todd, F. D., 3rd & Noyes, D. H. A behavioral and anatomical analysis of spinal cord injury produced by a feedback-controlled impaction device. *Exp Neurol* **95**, 548-570, doi:10.1016/0014-4886(87)90299-8 (1987).

6 Cermak, N. *et al.* Whole-organism behavioral profiling reveals a role for dopamine in state-dependent motor program coupling in C. elegans. *Elife* **9**, doi:10.7554/eLife.57093 (2020).

7 Iderberg, H. *et al.* NLX-112, a novel 5-HT1A receptor agonist for the treatment of L-DOPA-induced dyskinesia: Behavioral and neurochemical profile in rat. *Exp Neurol* **271**, 335-350, doi:10.1016/j.expneurol.2015.05.021 (2015).

8 Machado, A. S., Darmohray, D. M., Fayad, J., Marques, H. G. & Carey, M. R. A quantitative framework for whole-body coordination reveals specific deficits in freely walking ataxic mice. *Elife* **4**, doi:10.7554/eLife.07892 (2015).
9 Mathis, A. *et al.* DeepLabCut: markerless pose estimation of user-defined body parts with deep learning. *Nat Neurosci* **21**, 1281-1289, doi:10.1038/s41593-018-0209-y (2018).
10 Kabra, M., Robie, A. A., Rivera-Alba, M., Branson, S. & Branson, K. JAABA: interactive machine learning for automatic annotation of animal behavior. *Nat Methods* **10**, 64-U87, doi:10.1038/Nmeth.2281 (2013).
11 Ben-Shaul, Y. OptiMouse: a comprehensive open source program for reliable detection and analysis of mouse body and nose positions. *BMC Biol* **15**, 41, doi:10.1186/s12915-017-0377-3 (2017).
12 Pereira, T. D. *et al.* Fast animal pose estimation using deep neural networks. *Nat Methods* **16**, 117-125, doi:10.1038/s41592-018-0234-5 (2019).
13 Basso, D. M., Beattie, M. S. & Bresnahan, J. C. A sensitive and reliable locomotor rating scale for open field testing in rats. *J Neurotrauma* **12**, 1-21, doi:10.1089/neu.1995.12.1 (1995).
14 Wiltschko, A. B. *et al.* Mapping Sub-Second Structure in Mouse Behavior. *Neuron* **88**, 1121-1135, doi:10.1016/j.neuron.2015.11.031 (2015).
15 Berman, G. J., Choi, D. M., Bialek, W. & Shaevitz, J. W. Mapping the stereotyped behaviour of freely moving fruit flies. *J R Soc Interface* **11**, doi:10.1098/rsif.2014.0672 (2014).
16 Markowitz, J. E. *et al.* The Striatum Organizes 3D Behavior via Moment-to-Moment Action Selection. *Cell* **174**, 44-58, doi:10.1016/j.cell.2018.04.019 (2018).
17 Arac, A., Zhao, P., Dobkin, B. H., Carmichael, S. T. & Golshani, P. DeepBehavior: A Deep Learning Toolbox for Automated Analysis of Animal and Human Behavior Imaging Data. *Front. Syst. Neurosci.* **13**, 1-12 (2019).
18 Graving, J. M. *et al.* DeepPoseKit, a software toolkit for fast and robust animal pose estimation using deep learning. *eLife* **8**, e47994, doi:10.7554/eLife.47994 (2019).
19 Schamhardt, H. C., van den Bogert, A. J. & Hartman, W. Measurement techniques in animal locomotion analysis. *Acta Anat (Basel)* **146**, 123-129, doi:10.1159/000147433 (1993).
20 Mychasiuk, R., Harker, A., Ilnytskyy, S. & Gibb, R. Paternal Stress Prior to Conception Alters DNA Methylation and Behaviour of Developing Rat Offspring. *Neuroscience* **241**, 100-105, doi:10.1016/j.neuroscience.2013.03.025 (2013).
21 Jenkins, S., Harker, A. & Gibb, R. Maternal Preconception Stress Alters Prefrontal Cortex Development in Long-Evans Rat Pups without Changing Maternal Care. *Neuroscience* **394**, 98-108, doi:10.1016/j.neuroscience.2018.10.023 (2018).
22 Keyes, K. M., Davey Smith, G. & Susser, E. Associations of prenatal maternal smoking with offspring hyperactivity: causal or confounded? *Psychol Med* **44**, 857-867, doi:10.1017/S0033291713000986 (2014).
23 Bruin, J. E., Gerstein, H. C. & Holloway, A. C. Long-term consequences of fetal and neonatal nicotine exposure: a critical review. *Toxicol Sci* **116**, 364-374, doi:10.1093/toxsci/kfq103 (2010).
24 Zhu, J. *et al.* Prenatal nicotine exposure mouse model showing hyperactivity, reduced cingulate cortex volume, reduced dopamine turnover, and responsiveness to oral

methylphenidate treatment. *J Neurosci* **32**, 9410-9418, doi:10.1523/JNEUROSCI.1041-12.2012 (2012).

25 Zhu, J., Lee, K. P., Spencer, T. J., Biederman, J. & Bhide, P. G. Transgenerational transmission of hyperactivity in a mouse model of ADHD. *J Neurosci* **34**, 2768-2773, doi:10.1523/JNEUROSCI.4402-13.2014 (2014).

26 McCarthy, D. M. *et al.* Nicotine exposure of male mice produces behavioral impairment in multiple generations of descendants. *PLoS Biol* **16**, e2006497, doi:10.1371/journal.pbio.2006497 (2018).

27 Blood-Siegfried, J. & Rende, E. K. The long-term effects of prenatal nicotine exposure on neurologic development. *J Midwifery Womens Health* **55**, 143-152, doi:10.1016/j.jmwh.2009.05.006 (2010).

28 LeSage, M. G., Gustaf, E., Dufek, M. B. & Pentel, P. R. Effects of maternal intravenous nicotine administration on locomotor behavior in pre-weanling rats. *Pharmacol Biochem Behav* **85**, 575-583, doi:10.1016/j.pbb.2006.10.012 (2006).

29 Golani, I., Bronchti, G., Moualem, D. & Teitelbaum, P. Warm-up Along Dimensions of Movement in the Ontogeny of Exploration in Rats and Other Infant Mammals. *P Natl Acad Sci-Biol* **78**, 7226-7229, doi:DOI 10.1073/pnas.78.11.7226 (1981).

30 Golani, I. A Mobility Gradient in the Organization of Vertebrate Movement - the Perception of Movement through Symbolic Language. *Behav Brain Sci* **15**, 249-266, doi:Doi 10.1017/S0140525x00068539 (1992).

31 Eilam, D. & Golani, I. The ontogeny of exploratory behavior in the house rat (Rattus rattus): the mobility gradient. *Dev Psychobiol* **21**, 679-710, doi:10.1002/dev.420210707 (1988).

32 Ryait, H. *et al.* Data-driven analyses of motor impairments in animal models of neurological disorders. *PLoS Biol* **17**, e3000516, doi:10.1371/journal.pbio.3000516 (2019).

33 Szegedy, C., Vanhoucke, V., Ioffe, S., Shlens, J. & Wojna, Z. Rethinking the Inception Architecture for Computer Vision. *Proc Cvpr Ieee*, 2818-2826, doi:10.1109/Cvpr.2016.308 (2016).

34 Bach, S. *et al.* On Pixel-Wise Explanations for Non-Linear Classifier Decisions by Layer-Wise Relevance Propagation. *PLoS One* **10**, e0130140, doi:10.1371/journal.pone.0130140 (2015).

35 Lapuschkin, S. *et al.* Unmasking Clever Hans predictors and assessing what machines really learn. *Nat Commun* **10**, 1096, doi:10.1038/s41467-019-08987-4 (2019).

36 Zhou, F., Duh, H. B. L. & Billinghurst, M. Trends in Augmented Reality Tracking, Interaction and Display: A Review of Ten Years of ISMAR. *Int Sym Mix Augment*, 193-202 (2008).

37 De Ryck, M. & Teitelbaum, P. Morphine versus haloperidol catalepsy in the rat: an electromyographic analysis of postural support mechanisms. *Exp Neurol.* **79**, 54-76 (1983).

38 Singer, H. S. Motor stereotypies. *Semin Pediatr Neurol* **16**, 77-81, doi:10.1016/j.spen.2009.03.008 (2009).

39 Singer, H. S. Stereotypic movement disorders. *Handb Clin Neurol* **100**, 631-639, doi:10.1016/B978-0-444-52014-2.00045-8 (2011).

40 Martino, D. & Hedderly, T. Tics and stereotypies: A comparative clinical review. *Parkinsonism Relat Disord* **59**, 117-124, doi:10.1016/j.parkreldis.2019.02.005 (2019).

41 Berman, G. J. Measuring behavior across scales. *Bmc Biol* **16**, 23, doi:10.1186/s12915-018-0494-7 (2018).
42 Wolgin, D. L. Amphetamine stereotypy, the basal ganglia, and the "selection problem". *Behav Brain Res* **231**, 297-308, doi:10.1016/j.bbr.2011.11.003 (2012).
43 Lelard, T., Jamon, M., Gasc, J. P. & Vidal, P. P. Postural development in rats. *Exp Neurol* **202**, 112-124, doi:10.1016/j.expneurol.2006.05.018 (2006).
44 Eilam, D., Zor, R., Szechtman, H. & Hermesh, H. Rituals, stereotypy and compulsive behavior in animals and humans. *Neurosci Biobehav Rev* **30**, 456-471, doi:10.1016/j.neubiorev.2005.08.003 (2006).
45 Braitenberg, V. & Schüz, A. in *Cortex: Statistics and Geometry of Neuronal Connectivity* 135-137 (Springer, 1998).
46 Ancona, M., Ceolini, E., Oztireli, C. & Gross, M. Towards better understanding of gradient-based attribution methods for Deep Neural Networks. *6th International Conference on Learning Representations (ICLR 2018)* (2018).
47 Shrikumar, A., Greenside, P. & Kundaje, A. in *Proceedings of the 34th International Conference on Machine Learning* Vol. 70 (eds Precup Doina & Teh Yee Whye) 3145-3153 (PMLR, Proceedings of Machine Learning Research, 2017).
48 Hochreiter, S. & Schmidhuber, J. Long short-term memory. *Neural Comput* **9**, 1735-1780, doi:DOI 10.1162/neco.1997.9.8.1735 (1997).
49 Greff, K., Srivastava, R. K., Koutnik, J., Steunebrink, B. R. & Schmidhuber, J. LSTM: A Search Space Odyssey. *Ieee T Neur Net Lear* **28**, 2222-2232, doi:10.1109/Tnnls.2016.2582924 (2017).
50 Barnickel, T., Weston, J., Collobert, R., Mewes, H. W. & Stumpflen, V. Large scale application of neural network based semantic role labeling for automated relation extraction from biomedical texts. *Plos One* **4**, e6393, doi:10.1371/journal.pone.0006393 (2009).
51 Ji, S., Yang, M. & Yu, K. 3D convolutional neural networks for human action recognition. *IEEE Trans Pattern Anal Mach Intell* **35**, 221-231, doi:10.1109/TPAMI.2012.59 (2013).
52 Montavon, G., Orr, G. B., Müller, K.-R. & SpringerLink (Online service). in *Lecture Notes in Computer Science*, 1 online resource (XII, 769 p (Springer Berlin Heidelberg : Imprint: Springer,, Berlin, Heidelberg, 2012).
53 Krizhevsky, A., Sutskever, I. & Hinton, G. E. ImageNet Classification with Deep Convolutional Neural Networks. *Commun Acm* **60**, 84-90, doi:10.1145/3065386 (2017).
54 Szegedy, C. *et al.* Going Deeper with Convolutions. *2015 Ieee Conference on Computer Vision and Pattern Recognition (Cvpr)*, 1-9, doi:DOI 10.1109/cvpr.2015.7298594 (2015).
55 Ciresan, D., Meier, U. & Schmidhuber, J. Multi-column Deep Neural Networks for Image Classification. *2012 Ieee Conference on Computer Vision and Pattern Recognition (Cvpr)*, 3642-3649 (2012).
56 Collobert, R. *et al.* Natural Language Processing (Almost) from Scratch. *J Mach Learn Res* **12**, 2493-2537 (2011).
57 Le, Q. V., Zou, W. Y., Yeung, S. Y. & Ng, A. Y. Learning hierarchical invariant spatio-temporal features for action recognition with independent subspace analysis. *2011 Ieee Conference on Computer Vision and Pattern Recognition (Cvpr)* (2011).
58 Samek, W., Binder, A., Montavon, G., Lapuschkin, S. & Muller, K. R. Evaluating the Visualization of What a Deep Neural Network Has Learned. *Ieee T Neur Net Lear* **28**, 2660-2673, doi:10.1109/Tnnls.2016.2599820 (2017).

59 Alber, M. *et al.* iNNvestigate Neural Networks! *J Mach Learn Res* **20** (2019).
60 Lapuschkin, S., Binder, A., Montavon, G., Muller, K. R. & Samek, W. The LRP Toolbox for Artificial Neural Networks. *J Mach Learn Res* **17** (2016).
61 Srinivasan, V., Lapuschkin, S., Hellge, C., Muller, K. R. & Samek, W. Interpretable Human Action Recognition in Compressed Domain. *Int Conf Acoust Spee*, 1692-1696 (2017).
62 Samek, W., Wiegand, T. & Muller, K. R. Explanable Artificial inteligence: Understanding, visualizing and interpreting deep learning models. *ITU Journal: ICT Discoveries - Special Issue 1 - The Impact of Artificial Intelligence (AI) on Communication Networks and Services* **1**, 39-48 (2018).

Supplementary materials

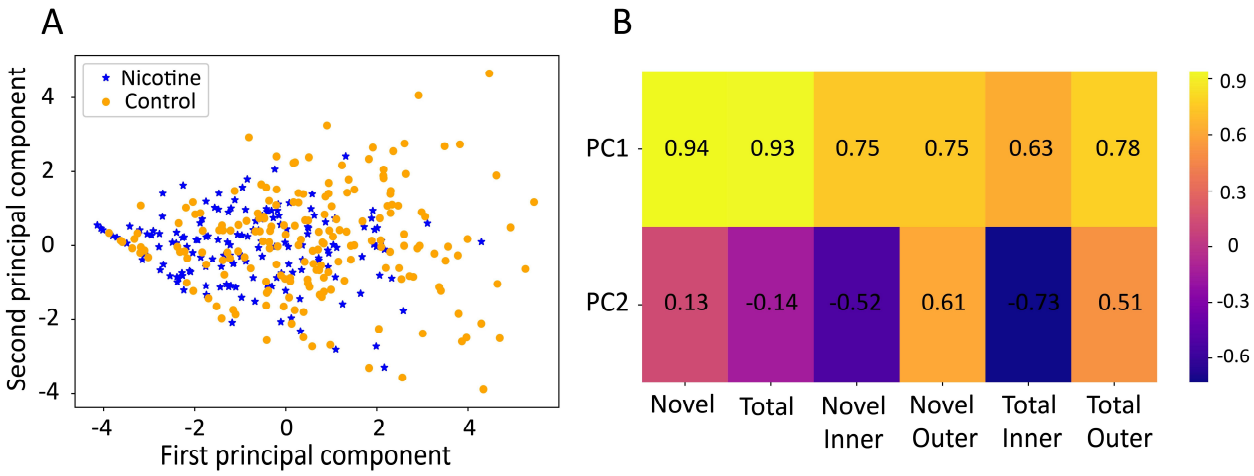

Suppl. Fig. 1: (A) Principal component (PC) space of behavioral measures. Each dot represents a single animal with MPNE group denoted in blue and control group in orange. Note that more control animals have high values of PC1 in comparison with the nicotine animals. To investigate it, we calculated the correlations between principal components and movement measures (B). We found that the first principal component has the largest correlation with the "Novel" and then with "Total" measure. This indicates that control animals have a greater tendency to explore new places (i.e. enter a greater number of unique squares) as well as to explore more (i.e. enter more squares overall) than MPNE animals.

A

RNN network architecture	Accuracy (% ± SEM)
One layer of LSTM with 256 neurons	87.5% ± 1.9%
One layer of LSTM with 400 neurons	86% ± 1.5%
One layer of LSTM with 512 neurons	86% ± 0.5%
Three layers of LSTM with (128, 64, 32) neurons	85.8% ± 1.2%
Two layers of LSTM with (256, 64) neurons	85.2%± 1.4%

B

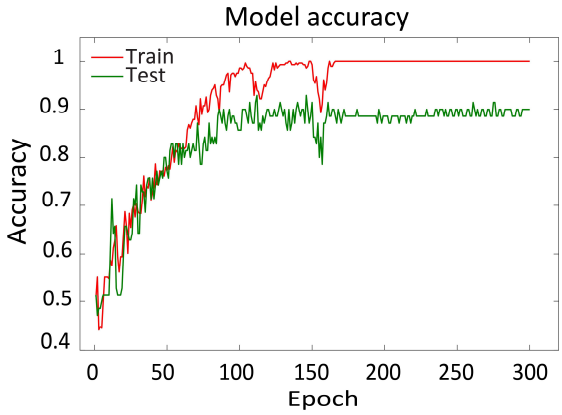

Suppl. Fig 2. (A) Different architectures of recurrent neural network (RNN) tested. For this manuscript we selected the top network (one layer of LSTM with 256 neurons). However, all tested networks produced similar results. This shows that our network does not need fine tuning to outperform machine learning methods using expert selected movement measures.

(B) Sample learning curve from training top RNN with one layer of 256 long short-term memory (LSTM)[48,49] units. Note that on training data we achieved 100% accuracy (red line), however on testing data accuracy was reduced (green line). This suggests that with larger dataset performance of the network may further improve.

Suppl. Text 1. ***Notes on knowledge extraction from neural networks***. Although deep neural networks have demonstrated impressive performance in complex machine learning tasks[50-57] and are key components of many critical decision or predictive processes, they have the disadvantage of acting as a black box, and so not providing information about the internal reasoning for how they reach a certain classification decision[34,58-61]. In an attempt to overcome this shortcoming, multiple analysis methods have been proposed to explain predictions of complex non-linear classifiers in terms of input variables[34,46,58,59]. One of the most powerful methods in this regard is

Layer-wise Relevance Propagation (LRP)[34], which we used here (Methods). LRP algorithms operate by propagating the prediction backward in the neural network and quantifying the "importance" of input components in classification decisions by attributing relevance scores to them. Video data contain both special (pixels) and temporal (frames) information, so the relevance data provide both special and temporal information about network decision making[61,62]. Special information showed us where the network was looking in the classification task[61]. This showed that the network is considering the difference in the behavior of control and MPNE animals in classification of video data rather than differences in irrelevant features that may vary between videos (e.g. position of the timer, orientation of the box, or glare from overhead lighting). Temporal information identifies the most relevant time points[62] in the behavior. Here, we present a general approach to analyze behavioral video data by identifying the most important spatio-temporal features used by the network for animal classification. This allows us to uncover in a data-driven way the behavioral components most affected by MPNE.

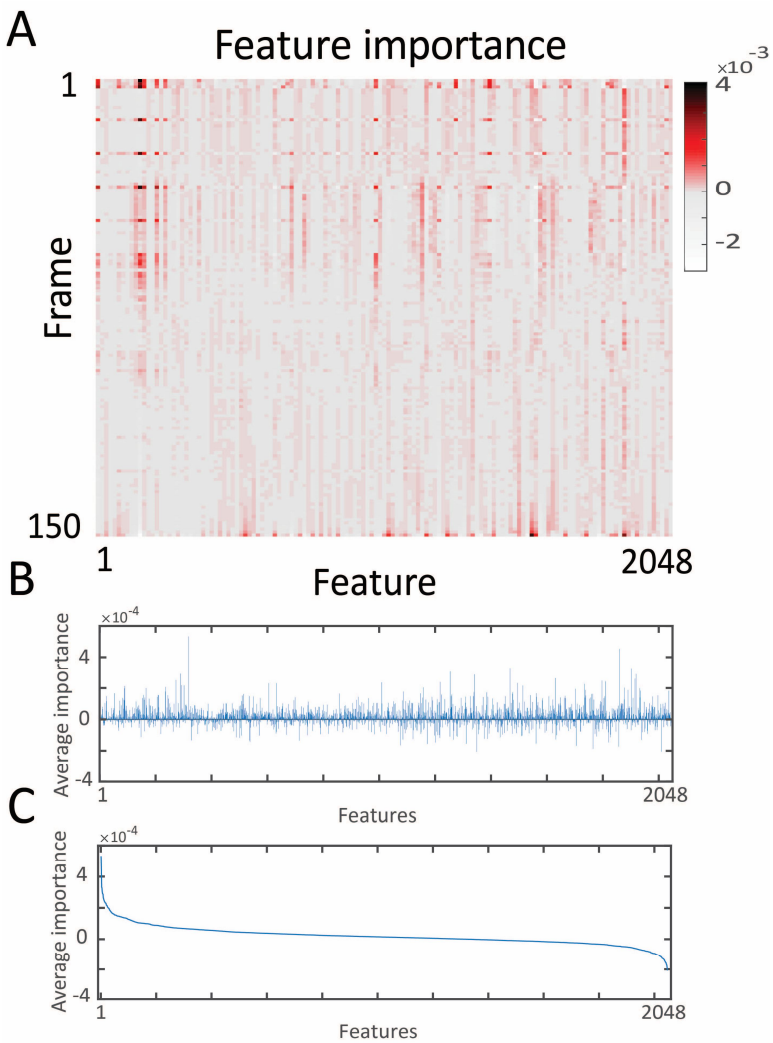

Suppl. Fig 3. Most informative features for network decisions. (A) Average of feature's importance over all videos, as shown in main text in Fig 3A. Considering reoccurring peaks in feature importance, it is apparent that the network is identifying periodic behavior, especially in the early 50 frames (~ 17 sec), to distinguish MPNE animals from control animals. Our RNN network was able to detect a repetitive pattern in the behavior because it is composed of the LSTM units which have memory and are specialized in identifying sequences of activity. (B) Average relevance (importance) of each 2048 features across all video data. Average relevance was obtained by averaging columns in the matrix shown in panel (A). (C) The same average feature importance as in (B), but sorted from highest to the lowest value. It illustrates that about 20 features had a disproportional effect on network decision making.

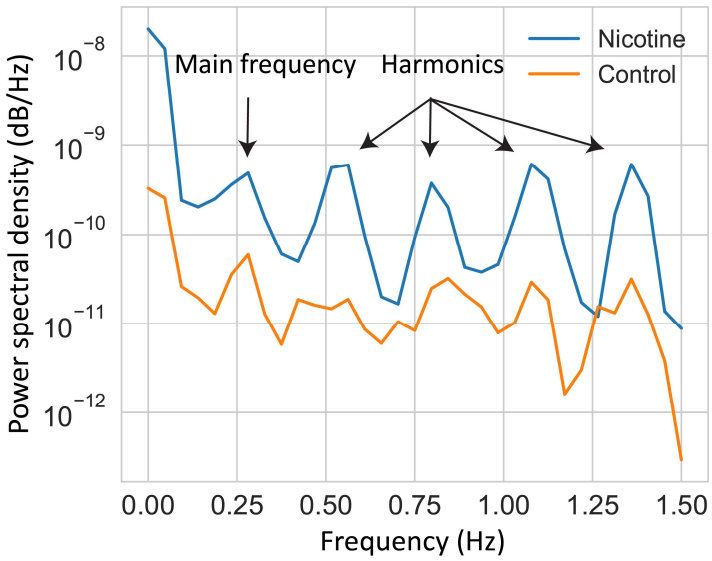

Suppl. Fig. 4. Power spectra analysis. In order to investigate periodic behavior shown in Fig. 3B, we calculated power spectra of the average feature importance. Blue and orange lines denote MPNE and control animals, respectively. Peak in power spectra at frequency of 0.27 Hz confirmed that video features oscillate with period of 1/0.27=3.7s. Note that this periodic behavior was seen mostly in MPNE animals. This indicates that MPNE animals have much more stereotypical behavior, while control animals have more diverse and less repetitive movements.

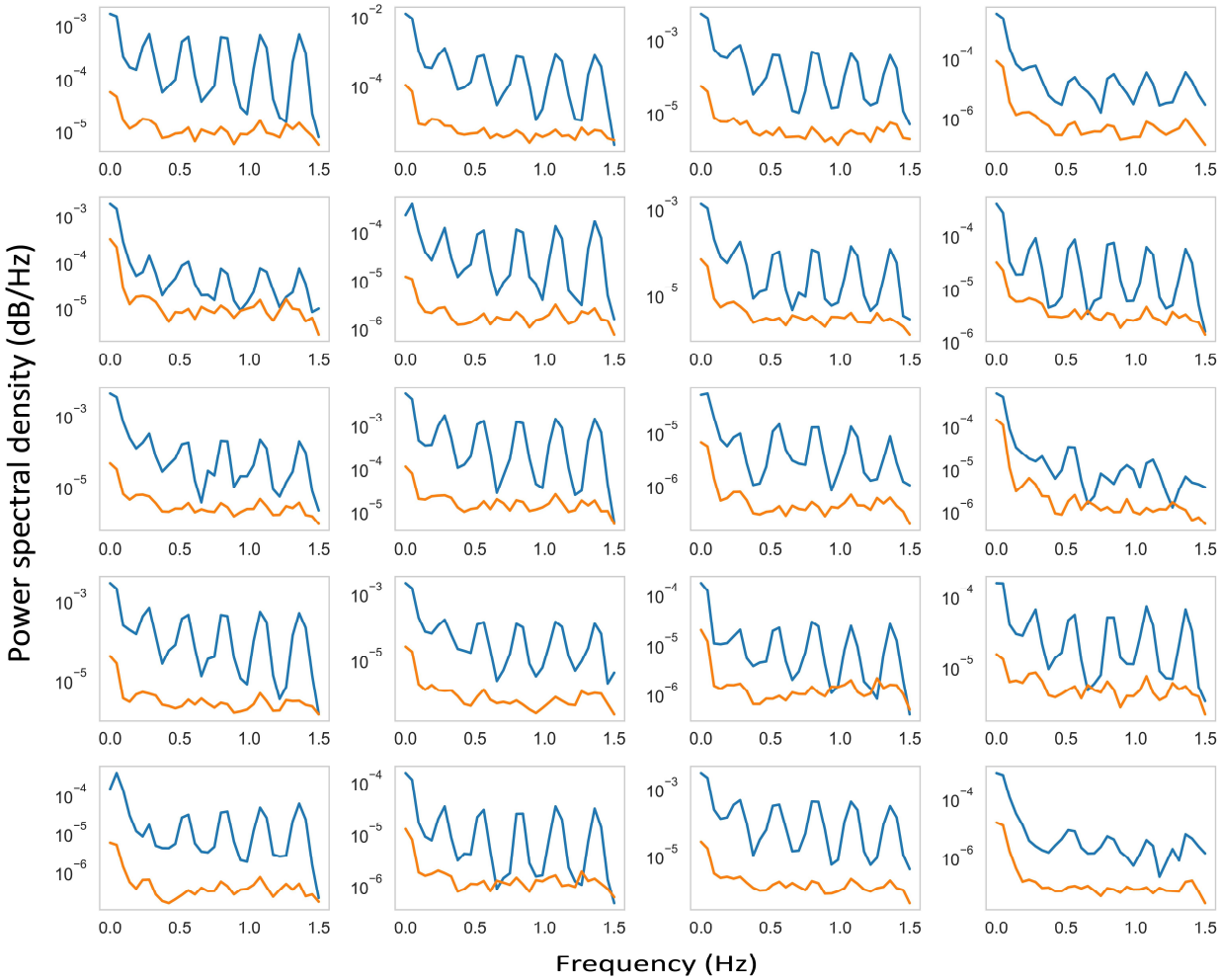

Suppl. Fig. 5. Power spectral analysis for 20 most important features. The blue and orange lines indicate MPNE and control animals, respectively. After identifying the most important features as illustrated in Suppl. Fig 3D, the power spectral for each of 20 top features was calculated in each video. Then, we averaged spectra of each feature, separately for MPNE and control animals, which lead to the 20 graphs shown above. As can be seen, the periodic behavior with the frequency of about 0.27 Hz is clearly visible in nearly all of the features.

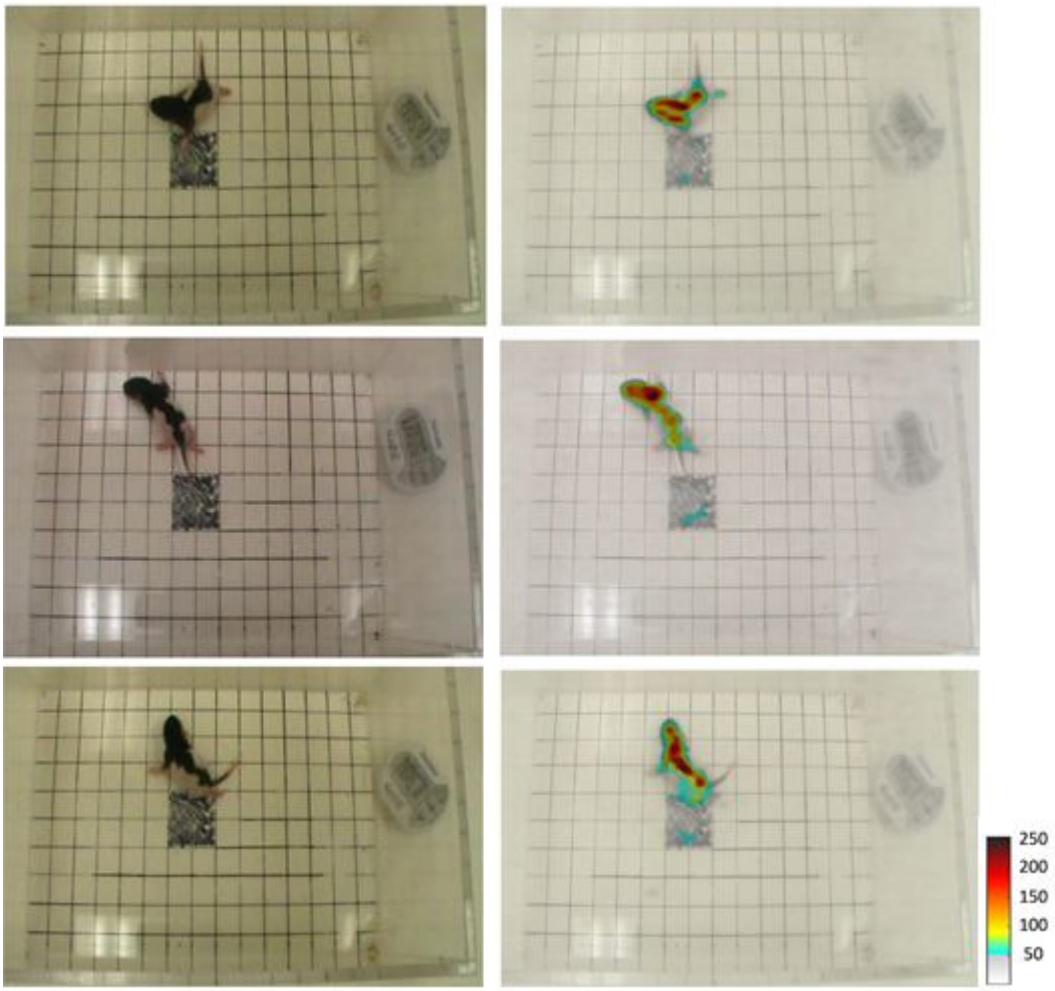

Suppl. Fig. 6: (Left column) Representative video frames, and the same frames with superimposed network focus (Right column). Frames illustrate the most informative pixels used by network to make decisions. This allowed us to verify that the network used features related to rat posture to discriminate control from MPNE animals. This analyses also ensures that the network does not 'cheat' by using spurious features like clock display. To superimpose pixel importance on the frames the values of importance were rescaled to range 50-250. The pixel importance was obtained by using LRP method described above. Using other methods like gradient*input methods[46,47] gave qualitatively similar results.